Northumbria Research Link

Citation: Wu, Jianhui, Yin, Changshuai, Zhou, Jian, Li, Honglang, Liu, Yi, Shen, Yiping, Garner, Sean, Fu, Richard and Duan, Huigao (2020) Ultrathin Glass-Based Flexible, Transparent, and Ultrasensitive Surface Acoustic Wave Humidity Sensor with ZnO Nanowires and Graphene Quantum Dots. ACS Applied Materials & Interfaces, 12 (35). pp. 39817-39825. ISSN 1944-8244

Published by: American Chemical Society

URL: https://doi.org/10.1021/acsami.0c09962 <https://doi.org/10.1021/acsami.0c09962>

This version was downloaded from Northumbria Research Link: http://nrl.northumbria.ac.uk/id/eprint/44254/

Northumbria University has developed Northumbria Research Link (NRL) to enable users to access the University's research output. Copyright © and moral rights for items on NRL are retained by the individual author(s) and/or other copyright owners. Single copies of full items can be reproduced, displayed or performed, and given to third parties in any format or medium for personal research or study, educational, or not-for-profit purposes without prior permission or charge, provided the authors, title and full bibliographic details are given, as well as a hyperlink and/or URL to the original metadata page. The content must not be changed in any way. Full items must not be sold commercially in any format or medium without formal permission of the copyright holder. The full policy is available online: http://nrl.northumbria.ac.uk/policies.html

This document may differ from the final, published version of the research and has been made available online in accordance with publisher policies. To read and/or cite from the published version of the research, please visit the publisher's website (a subscription may be required.)

Northumbria University NEWCASTLE

University Library

Ultra-thin Glass Based Flexible, Transparent and Ultra-sensitive Surface Acoustic Wave Humidity Sensor with ZnO Nanowires and Graphene Quantum Dots

Jianhui Wu,[‡a] Changshuai Yin,[‡a] Jian Zhou,[*a] Honglang Li,[b] Yi Liu,[a] Yiping Shen,[c] Sean Garner,[d] Yongqing Fu,[e] Huigao Duan.[a]

a. Engineering Research Center of Automotive Electrics and Control Technology, College of Mechanical and Vehicle Engineering, Hunan University, Changsha 410082, P.R. China

b. CAS Center for Excellence in Nanoscience, National Center for Nanoscience and Technology, Beijing 100190, P.R. China

c. Hunan Provincial Key Laboratory of Health Maintenance for Mechanical Equipment, Hunan University of Science and Technology, Xiangtan 411201, P.R. China

d. Corning Research & Development Corporation, One River Front Plaza, Corning, NY 14831, USA

e. Faculty of Engineering and Environment, Northumbria University, Newcastle upon Tyne, NE1 8ST, United Kingdom

KEYWORDS: flexible glass; ZnO; flexible SAW; ZnO NWs & GQDs; humidity sensors

Supporting Information Placeholder

ABSTRACT: Flexible electronic devices are normally based on organic polymer substrate. In this work, ultra-thin glass based flexible, transparent and ultra-sensitive ZnO/glass surface acoustic wave (SAW) humidity sensor is developed using a composite sensing layer of ZnO nanowires (NWs) and graphene quantum dots (GQDs). It shows much larger effective electromechanical coupling coefficients and signal amplitudes, compared with those of flexible polymer based SAW devices reported in literature. Attributed to large specific surface areas of ZnO NWs, large numbers of hydrophilic functional groups of GQDs, as well as the formation of p-n heterojunctions between GQDs and ZnO NWs, the developed ZnO/glass flexible SAW sensor shows an ultra-high humidity sensitivity of 40.16 kHz/%RH, along with its excellent stability and repeatability. This flexible and transparent SAW sensor has demonstrated insignificant deterioration of humidity sensing performance, when it is bent on a curved surface with a bending angle of 30°, revealing its potential applications for sensing on curved and complex surfaces. The humidity sensing and human breathing detection have further been demonstrated for wearable electronic applications using ultra-thin glass based devices with completely inorganic materials.

Introduction

Humidity or moisture levels are constantly monitored in respiratory equipment, sterilizers, incubators and pharmaceutical processing in medical fields, wafer processing for manufacturing integrated circuits industry, green-house air-conditioning, and soil moisture monitoring in agriculture.[1] Recently, flexible (or possibly transparent) humidity sensors have become a hot research topic, as they can be integrated into human-machine interface and electronic skin to monitor robots' performances and human health.[2-6] For example, a flexible humidity sensor was used for the non-contact finger-tip moisture detection and human breathing rate detection.[7] Monitoring the hydration levels of the skin allows for the evaluation of various human physiological conditions which can be related to athletic performance,[2] aging process,[8] and healing condition of wounds.[4] For most of these applications, humidity sensors are needed to be flexible, or bendable, or even wearable, and in some cases, transparent, along with the most critical requirement, e.g., high sensitivity.

Surface acoustic wave (SAW) devices are one of the major building blocks for electronics,[9] microsensors,[10-11] and microsystems.[12] SAW-based humidity sensors have been extensively investigated owing to their high sensitivity, small size, and ability to be interfaced with passive wireless systems. However, conventional SAW humidity sensors are usually based on bulk and rigid substrates such as quartz [13-15], $LiNbO_3$ [16], ZnO or AlN films on rigid Si or glass substrates,[17] which make sensors incompatible with curved surfaces of flexible electronics. Luo's group recently developed ZnO/polymer flexible SAW humidity sensors with a sensitivity up to 3.47 kHz/%RH [18] and applied this type of device as a respiration sensor for monitoring obstructive sleep apnea syndrome.[19] However, because of the significant dissipation of sound waves and energy, and poor adhesion of thin films on these polymer substrates, they found that it is a great challenge to use these polymer-based thin film SAW devices for high-performance sensing, microfluidics and lab-on-a-chip applications.[20] Tao et al. further used aluminum foils/sheets as the substrate to make flexible SAW devices for various sensing (including humidity) and respiration monitoring.[21] However, it is well-known that these Al foil/sheet substrates are easily plastically deformed without a good flexibility, thus often unable to easily recover to their original states when they have been bent. Therefore, at present, there is still great challenge

to develop flexible SAW devices with high performance and good flexibility, for flexible lab-on-a-chip applications.

On another matter, to improve the sensitivity of the flexible humidity sensors, one of the commonly used solutions is to apply a functional layer of nano- and micro-structured networks which could achieve large surface-to-volume ratios and superior physical/chemical properties.[22-23] For example, Xuan et al.[24] reported SAW humidity sensors which used graphene oxide (GO) as a sensing layer, and achieved a sensitivity of 35.29 kHz/%RH. Le et al.[25] applied a uniform GO layer on the SAW device to achieve a sensitivity of 25.3 kHz/%RH. However, when these two-dimensional materials were applied as the sensitive layer onto the SAW devices, they were often simply attached to the device surface. They did not form a variety of spatial 3D structures, and could not significantly increase the number of active sites in the limited sensing area of the SAW devices. Other sensing layers such as metal-semiconductor oxides have been studied, but they often face the problems of long response time and large hysteresis, or sometimes, low sensitivity.[18] To improve the sensitivity of the metal oxide film-based SAW device, these semiconductor layers are often needed to be quite thick. However, a small number of water molecules will easily diffuse into this sensing layer through the boundaries of grains or defects, but cannot be released easily, which could be the reason for the significant increases in the response time and hysteresis.[18]

To solve these critical issues, in this work, we propose a flexible SAW humidity sensor based on a ZnO/flexible glass layered structure and use ZnO nanowires (NWs) and graphene quantum dots (GQDs) to form a composite sensing layer. We then systematically investigate their acoustic-electro coupling coefficient, humidity sensitivity, stability, and flexibility on a curved surface.

In our new sensing layer design on the flexible SAW device (as illustrated in Figure 1(a)), the GQDs with tunable sizes are uniformly mixed and integrated into the nanostructures of ZnO NWs, which can effectively combine the advantages of both these nanomaterials. We propose that there are several reasons for the significantly increased sensitivity using the ZnO NWs and GQDs composite sensing layer:

(1) Compared with a standard ZnO film, application of ZnO nanowires can increase the specific surface areas, which provide more active sites and can adsorb more water molecules during humidity sensing;[26]

(2) The GQDs synthesized by carbonization of citric acids have a larger density of hydrophilic functional groups such as carboxyl groups, which can significantly enhance the ability to adsorb water molecules;[27]

(3) Adding the GQDs can enhance the adsorption capacity of ZnO to water molecules due to the formation of these p-n heterojunctions, as the GQDs can be considered as a p-type semiconductor,[27] while the ZnO as an n-type semiconductor. The Fermi levels of ZnO NWs and GQDs are quite different, and the electrons in ZnO will be easily transferred to GQDs (Figure 1(a)), until the Fermi energy equilibrium is reached.[28-29] As a result, the ionized oxygen species (such as O^- and O^{2-}) will compete with the hydroxyl group for the active site on the surface of ZnO. The electron transfer at the heterojunction will reduce the number of ionized oxygen[30] and promote the reaction process of water molecules and oxygen ions to form hydroxyl groups.[31] This will increase the number of hydroxyl groups and improve the ability of the sensing layer to adsorb water molecules.

Experimental Section

The SAW devices were fabricated on flexible Corning® Willow® glass substrates (100 μm thick, and 100 mm in diameter) as illustrated in Figure 1b(i). Compared with flexible polymer substrate, ultra-thin glass is an inorganic material, with good mechanical and physical properties, including good thermal capability with its service temperature up to ~600 ℃. In addition, the flexible glass can be produced in wafer-level (up to 6-inch scale), suitable for fabricating flexible sensors in a large scale. Finally, it has good optical quality, environmental stability, significantly less acoustic wave damping as well as high smoothness (with a surface roughness much smaller than 0.5 nm), which are all very suitable for fabrication and application of flexible electronics device.

Piezoelectric ZnO films were deposited onto the flexible glass substrates using a direct-current (DC) magnetron sputtering system with a pure zinc target and an O_2/Ar mixture gas. The optimal deposition conditions were found to be: substrate temperature of 100°C, chamber gas pressure of 2 Pa, O_2/Ar of 50/100 sccm, DC sputtering power of 200 W and a bias voltage of −75 V. Figure 1b(ⅱ) shows a photo of ZnO film-coated flexible glass, demonstrating its good flexibility. Crystalline structures of the deposited films were analyzed using X-ray diffraction (XRD-6000) with a Cu-$K\alpha$ radiation source and a scanned angle of 2θ =20°~70°. The c-axis orientation of the crystals was verified from the strong diffraction peak of ZnO (0002). Crystallite sizes of the ZnO were calculated from the Debye–Scherrer formula based on the full width at half maximum (FWHM) of the ZnO (002) diffraction peak (β in radians):[32-33] $D = K\lambda / (\beta \cos\theta)$, where K is the shape factor of the average crystallite with a value of 0.94, λ the X-ray wavelength (1.5405 Å for Cu target), θ the Bragg angle, and D the mean crystallite gain size normal to diffracting planes. Film residual strain was calculated from $\varepsilon_z = (c - c_0) / c_0$,[34] where c_0 is the strain-free lattice constant (4.979 Å) and c the lattice constant which is equal to twice of the inter-planar spacing d, measured from the position of the (002) peak using the Bragg equation. Scanning electron microscope (SEM, ZEISS Sigma-300) and atomic force microscope (AFM, Dimension Icon, Bruker) were used to obtain cross-sectional microstructure and surface topography of the deposited film, respectively.

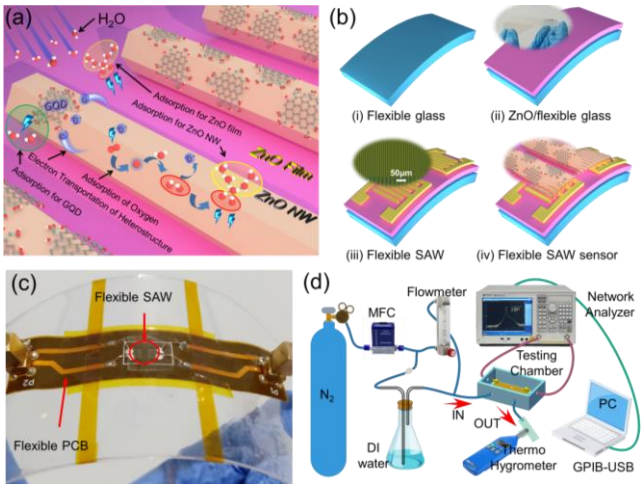

Figure 1. (a) Schematic illustration of the adsorption mechanism of H_2O molecules on the composite sensing layer; (b) Schematic diagram of the fabrication process for the SAW

Sample	f_r [MHz]	Sensitivity [kHz/%RH][a)]	Surface Treatment
D1	220.2	2.37	clean surface without sensing layer
D2	169.63	1.11	clean surface without sens-ing layer
D3	138.35	0.24	clean surface without sens-ing layer
D4	220.05	4.61	ZnO NWs and low con-cen-tration GQDs (0.1mg/ml)
D5	169.4	2.63	ZnO NWs and low con-centration GQDs (0.1mg/ml)
D6	138.35	1.17	ZnO NWs and low con-centration GQDs (0.1mg/ml)
D7	219.64	40.16	ZnO NWs and high con-centration GQDs (2mg/ml)
D8	169.44	38.43	ZnO NWs and high con-centration GQDs (2mg/ml)
D9	138.35	21.24	ZnO NWs and high con-centration GQDs (2mg/ml)

sensor based on ZnO NWs and GQDs; (c) Device packaged on polyimide flexible PCB board and mounted on 1 mm thick PET; (d) A schematic view of the testing system used for humidity sensing.

UV photolithography and lift-off processes were used to fabricate two-port SAW resonators on the ZnO coated flexible glass with the gold (Au) interdigital transducers (IDTs) with different wavelengths (λ) of 12, 16 and 20 μm. The flexible SAW device has 50 pairs of IDTs with metallization ratios of 0.5, 100 pairs of reflectors, an aperture length of 200 λ, and the center distance between the two ports of 150 λ. Figure 1b(iii) shows a schematic drawing and an optical microscopy image of the fabricated flexible SAW device with a layered structure of Au/ZnO/flexible glass.

A mixed solution of ZnO NWs and GQDs (fabricated with the process shown in Figure S1 and the parameters listed in Table S1) was dripped onto the entire surface of the SAW device, and dried on a hot plate at 80℃, as schematically illustrated in Figure 1b(iv). Raman spectra of this layer were obtained using a Raman system (Alpha 300R, Witec), with a laser wavelength of 532 nm. Element composition and mapping analysis were performed using an energy dispersive spectroscopy (EDS) analyzer (Aztec X-Max^N 20 Oxford instruments). The detailed preparation procedures and the changes in surface morphology of ZnO NWs and GQDs are shown in Figures S1 and S2.

Figure 1(c) demonstrates the flexibility of the fabricated SAW devices. They were diced into a die from the glass wafer, and then packaged onto the flexible polyimide film printed circuit board (PCB) using adhesive. This polyimide PCB was then mounted onto a 1 mm thick polyethylene terephthalate (PET) support. The device's performance such as transmission characteristics were measured using an E5071C vector network analyzer. For the humidity sensing, the SAW device was placed inside an aluminum box with a volume of 136×72×35 mm^3 as shown in Figure 1(d). The nitrogen gas was controlled to flow through a water bottle, and different humidity environments were achieved by controlling the nitrogen flow rate of a glass rotor flow meter. The humidity level was calibrated using a standard thermo hygrometer. During the entire testing process, the temperature was maintained at ~20℃. A LabVIEW program was developed to implement automated measurements to record the frequency changes as a function of time at different relative humidity (RH) levels. Samples for humidity sensing were classified into three groups, D1-D3, D4-D6, D7-D9, and each group's sensors are consisted of SAW devices with wavelengths of 12 μm, 16 μm, and 20 μm and different treated surfaces, as listed in Table 1.

Table 1. Summary of the different SAW sensors with different treated surfaces.

[a)] the sensitivity at 80%RH.

Results and Discussion

Figure 2(a) shows the XRD pattern of the ZnO film, with a single large peak at the angle of 34.2°, corresponding to the ZnO (0002) crystal orientation. The full width at half maximum (FWHM) of the XRD curve of the deposited ZnO film is 0.117°, corresponding to the calculated mean grain size of about 71.07 nm. The axial stress was estimated to be 45.71 MPa calculated from the lattice constant obtained through XRD patterns, showing that the deposited film has a low residual stress on the flexible glass substrate. Figure 2(b) is a cross-section SEM image of the ZnO film (with a thickness of ~2.7 μm).The film has columnar structures of the ZnO nanocrystals perpendicular to the substrate. Figure 2(c) shows the surface morphology and roughness of the film measured using AFM. The root mean square (RMS) roughness was measured to be 6.14 nm over an area of 4×4 μm^2. Figure 2(d) shows an SEM image for the composite layer of ZnO NWs and GQDs materials on ZnO/flexible glass substrate. Although the GQDs were not obviously identified from the SEM image, it can be verified from the Raman spectrum in Figure 2(e). For the pure GQDs, two distinct peaks at 1350 cm^{-1} and 1580 cm^{-1} can be observed, which are assigned to the D peak and G peak, respectively.[35-36] For ZnO NWs, the peaks at 434 cm^{-1} and 1150 cm^{-1} are ascribed to the acoustic overtone of E_{2H} and the optical overtone of ZnO, repectively.[37] Results showed that The Raman spectra of the ZnO nanowire/GQDs have the main characteristic peak of GQDs, demonstrating the existence of GQDs. Figure 2(f) shows elements' distribution in the composite layer of ZnO NWs and GQDs, obtained using the EDS. Results reveal that the GQDs (e.g., element of carbon) are indeed coated on the ZnO NWs. We have also measured the average diameter and length of the ZnO NWs (see Figure S2) and calculated the specific surface area of ZnO NWs, which is ranged from 11.56 to 26.35 cm^2 (Table S2).

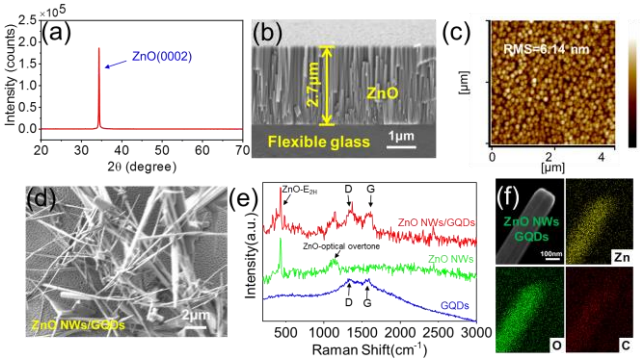

Figure 2. Characterization of ZnO thin film deposited on the flexible glass substrate and sensitive composite film: (a) XRD pattern of the ZnO layer; (b) SEM image of the cross-section of ZnO layer; (c) AFM image of ZnO layer; (d) SEM image of sensitive composite film dripped on the flexible device; (e) Raman spectra of pure GQDs, ZnO nanowire and ZnO nanowire/GQDs; (f) Element mapping of Zn, O, C elements in ZnO NWs and GQDs composite, revealing that the GQDs are indeed coated on the ZnO NWs.

Figure 3 shows the transmission (S_{21}) and reflection spectra (S_{11}) of flexible SAW devices with different wavelengths. All these flexible SAW devices show well-defined resonant peaks, corresponding to those of the Rayleigh waves. The resonant frequencies are 220.2, 169.63 and 138.35 MHz for the SAW devices with wavelengths of 12 μm, 16 μm, and 20 μm, respectively. The phase velocities (v_p) of these SAW devices, $v_p = \lambda f$, were calculated to be 2642.4, 2714.1, and 2767.0 m·s^{-1}, respectively, increasing gradually with an increase in wavelength from 12 μm to 20 μm. The phase velocity for the Rayleigh wave in an ideal (0002) ZnO crystal is ~2600 m·s^{-1}, depending on the crystal quality and deposition method used.[20] The phase velocity for the Rayleigh wave in the glass is 3200 m·s^{-1}, much larger than that of the ZnO film. When the wavelength is increased, more energy is dispersed in the flexible glass which has a higher velocity of wave propagation, thus leading to a higher velocity of the layered structure. The effective electromechanical coupling coefficients (K^2) obtained using the Smith-Chart Function of the network analyzer are 3.32%, 3.49 %, 3.31 % for the SAW devices with wavelengths of 12 μm, 16 μm and 20 μm,

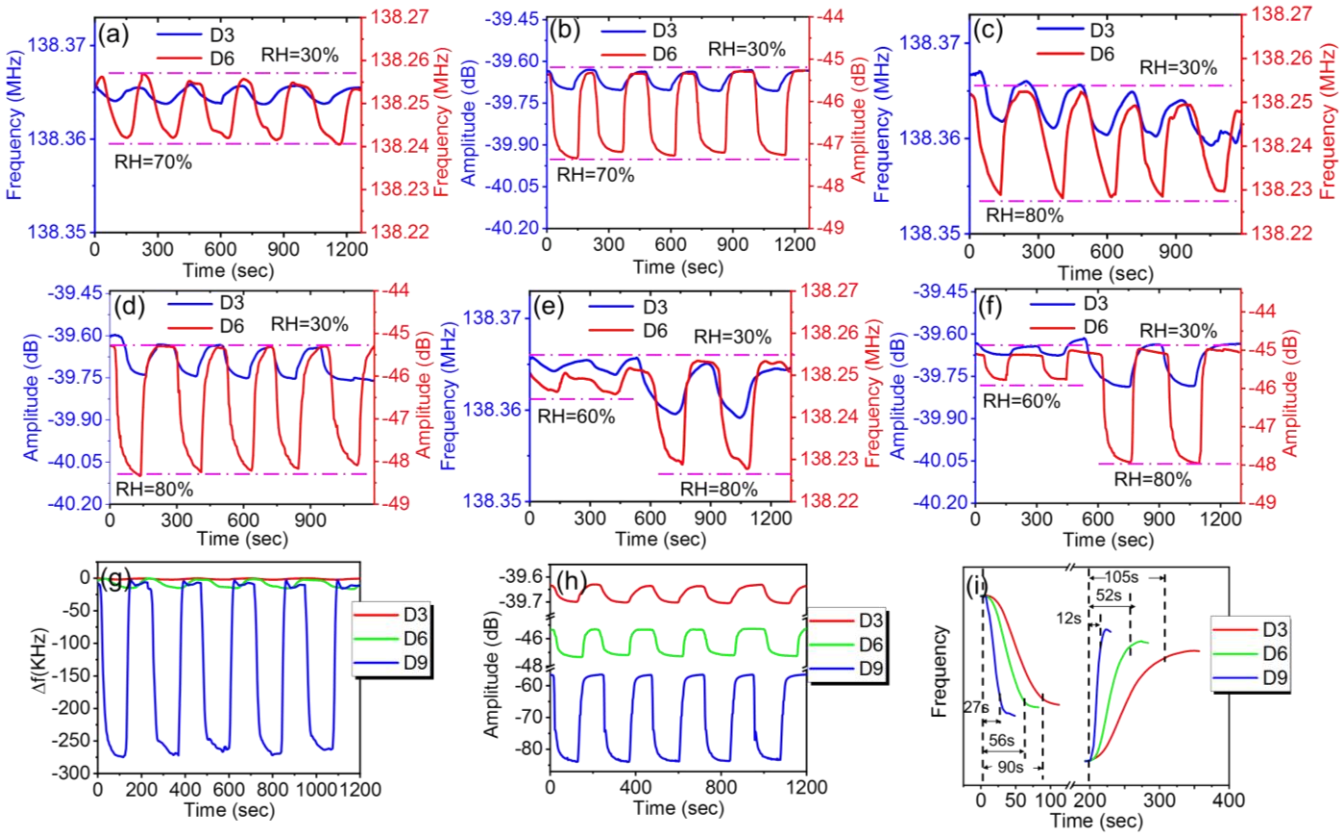

Figure 4. (a)&(b) Frequency and insertion loss characteristics of the sensors (D3, D6) with the humidity changed from 30%RH to 70%RH for 5 cycles; (c)&(d) Frequency and insertion loss characteristics of the sensors (D3, D6) with the humidity changed from 30%RH to 80%RH for 5 cycles; (e)&(f) Frequency and insertion loss characteristics of the sensors (D3, D6) with the humidity changed from 30%RH to 60%RH for two cycles and then changed from 30%RH to 80%RH for two cycles; (g)&(h) Comparison of frequency and insertion loss shifts for the sensors (D3, D6 and D9) based on different sensitive layers, with the humidity changed from 30%RH to 70%RH; (i) Response and recovery time of three SAW sensors (D3, D6, and D9) based on different sensitive layers, when the humidity level was changed from 30%RH to 70%RH.

respectively. The amplitude of the transmission signal of the flexible ZnO/glass SAW device is ~45 dB, which is much higher than those of previously reported flexible SAW devices on the polymer [12] and metallic foil substrate.[21]

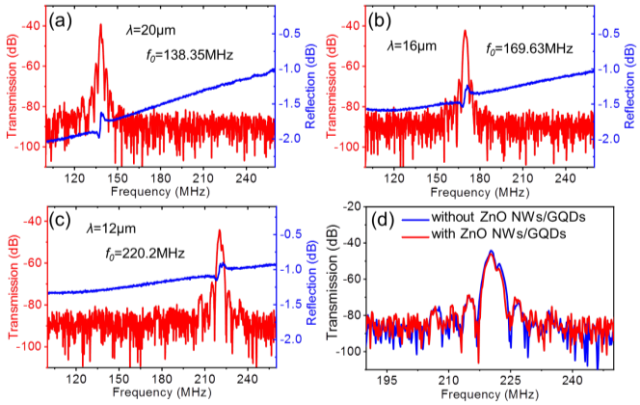

Figure 3. Transmission (S_{21}, red lines) and reflection (S_{11}, blue lines) spectra of the flexible ZnO SAW devices with a 2.7 μm thick ZnO film as a function of wavelength λ: (a) λ=20 μm; (b) 16 μm; (c) 12 μm; (d) typical transmission spectra of the SAW sensors (λ=12 μm) before and after ZnO NWs and GQDs coating.

Figure 3(d) shows the transmission spectra of SAW devices with a wavelength of 12 μm, with or without adding the humidity sensing layer. Results showed that after adding the sensitive layer, the resonant frequency and signal amplitude of the device remain nearly unchanged, which are suitable for humidity sensing tests.

ZnO is a hydrophilic material and water molecules can be easily absorbed by the ZnO layer of the device in a humid environment.[38] This induces a mass loading on the device surface, which influences the transmission characteristics of the SAW device. This is the sensing principle of ZnO film based SAW humidity sensors. Figure 4(a) shows the variation of the resonant frequency of the flexible SAW device (D3 listed in Table 1) with a λ=20 μm and without adding any sensing layer, when the relative humidity was changed from 30% to 70% for five cycles. The resonant frequency returns to the original value without any apparent saturation or hysteresis observed when the humidity level was decreased from 70%RH to 30%RH. The resonant frequency shift of D6 (listed in Table 1) is increased by 7 times compared with that of D3, which is due to the addition of the sensing layer on the SAW device. The results also show that the ZnO/glass flexible SAW devices have good humidity sensing performance and good repeatability.

The changes in the humidity level also influence the insertion loss of the SAW sensors, as shown in Figure 4(b). The reason for the decreases in insertion loss ($\Delta\alpha$) is due to the changes in

surface capacitance C_s, which is due to the loading of water molecules. The values of $\Delta\alpha$ can be calculated using:[39]

$$\frac{\Delta\alpha}{K} = \frac{k^2}{2}\frac{v_0 C_s \sigma_s}{\sigma_s^2 + (v_0 C_s)^2} \quad (1)$$

where K, σ_s, and v_0 are the acoustic vector, the sheet conductivity, and the original phase velocity, respectively. When the composite layer of ZnO NWs and GQDs is added to the flexible SAW device, the insertion loss is increased by 25 times when the relative humidity is changed from 30% to 70% and then back to 30%. It has a similar trend when the relative humidity is changed from 30% to 80% and back to 30% in five cycles as shown in Figures 4(c) and 4(d). These results demonstrate that this composite sensing layer of ZnO NWs and GQDs can enhance the humidity sensitivity of the flexible SAW devices.

Figures 4(e) and 4(f) show the changes of insertion loss and resonant frequency for the flexible sensor at various humidity levels. When the ambient humidity is increased from 30% to 60% and back to 30% for two cycles and then increased from 30% to 80% and back to 30% for two cycles, the flexible device shows a good stability without any saturation. The flexible SAW devices with ZnO NWs and GQDs composite layer show a much higher humidity sensitivity if compared with those SAW devices without this composite sensing layer.

To further investigate the effect of GQDs concentrations in the composite layer on the sensing performance of the flexible SAW device, we prepared different contents of GQDs into the composite sensing layers. Figures 4(g) and 4(h) compare the obtained resonant frequencies and insertion loss changes for the sensors with high concentrations of GQDs and low concentrations of GQDs, when the humidity level was changed from 30%RH to 70%RH. Obviously, there are significant frequency shifts and changes in the insertion loss when the concentration of GQDs is increased in the sensing layer. Figure 4(i) shows the response time and recovery time of three SAW sensors (e.g., D3, D6, and D9 as listed in Table 1) based on different sensitive layers, when the humidity level was changed from 30%RH to 70%RH. Results showed that adding the ZnO NWs and GQDs composite sensing layer can significantly decrease the response time and recovery time of the SAW humidity sensors.

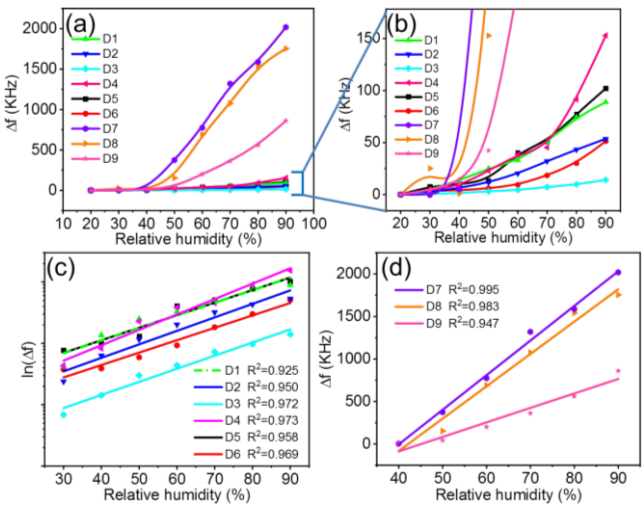

Figure 5. (a) The resonant frequency shifts as a function of relative humidity for sensors with different surface treatments; (b) an enlarged picture of (a); (c) the change of frequency as an exponential function of relative humidity; (d) the change of frequency as a linear function of relative humidity; (R^2 is the correlation coefficient).

During this test, the testing environment parameters such as temperature and pressure are precisely controlled in order not to affect the humidity sensing results. At such high frequencies (for example above 20 MHz), the resistance of film has little changes,[26] and the adsorbed water molecules cannot be effectively polarized and the dielectric phenomenon does not easily occur.[40-41] Therefore, in this study, the main reason for the frequency shift of SAW sensors based on the ZnO film is the mass loading effect.[42]

To investigate the performance of SAW sensors under different ranges of RHs, the frequency signals of the SAW sensor was measured with the RHs changed from 20% to 90% at a step of 10% RH. Figure 5(a) summarizes the data of the resonant frequency changes as a function of humidity levels for the sensors of D1 to D9 with various resonant frequencies.

Generally, the resonant frequencies of the SAW sensors change with the increase of humidity with a nonlinear characteristic, or an exponential relationship for all the sensors tested, similar to those reported in literature.[18] This can be described by the following relationship,

$$\ln(f - f_0) = \mathrm{A}(RH - \mathrm{RH}_0) + \mathrm{B} \quad (2)$$

where f_0 is the initial resonant frequency, RH_0 is the reference relative humidity, A and B are two coefficient constants. The relationship between the log function of frequency shift and relative humidity shows an excellent linearity ($0.925<R^2<0.995$) for all the sensors, as illustrated in Figure 5(c). However, when the quantum dots concentration is increased, the frequency offset changes linearly with the relative humidity at the range of 40%-90%, as can be seen from Figure 5(d). This may be due to the synergic effect of a large number of graphene quantum dots and ZnO nanowires strengthened by the formed heterojunctions, which can result in an improved sensing performance at this humidity level. A similar linear behavior has also been reported for the humidity sensing using the silver nanoparticles as sensitive membranes.[16]

The sensitivity (S) of a humidity sensor is generally defined as:

$$S = \frac{|\Delta f|}{\Delta RH} \quad (3)$$

where Δf and ΔRH are the frequency shifts and humidity changes, respectively. Based on Equation 3, the humidity sensitivity of all the tested sensors can be calculated and the results are summarized in Table 1. For a fixed frequency of 138.35 MHz (D3, D6 and D9), the sample D9 with a higher concentration of GQDs exhibits a sensitivity which is 18 times higher than that of the SAW device with a lower concentration of GQDs, and 88 times larger than that of ZnO flexible SAW sensors (without the composite sensing layer) at 80%RH. This demonstrates that the composite layer can significantly enhance the sensitivity, especially at a higher concentration of GQDs. Similarly, the devices with a frequency of 169.63 and 138.35 MHz have the similar trends of the results.

The resonant frequency of the SAW sensor has also shown a significant effect onits sensitivity, and the sensitivity of the sensor increases as the resonant frequency increases. In general, the frequency change, Δf, induced by an increased loaded mass, Δm, can be expressed as,[18]

$$\Delta f = \frac{C f_r^2}{A} \Delta m \qquad (4)$$

Table 2. Comparisons of sensitivities of different SAW-based humidity sensors.

Year	Structure	Sensing material	Flexibility	f [MHz]	Sensitivity [KHz/%RH][b)]	Ref.
2010	ST-quartz	silicon-containing polyelectrolyte	rigid	433	0.4	13
2013	ZnO/PI	ZnO layer	flexible	132.08	3.47	18
2014	$LiNbO_3$	Silver nanostructures	rigid	123.6	23.12	16
2015	ZnO/PI	Graphene oxide layer	flexible	395	35.29	24
2018	AlN/Si(doped)	GO	rigid	392	42.08	43
2019	ST-quartz	polyvinyl alcohol and nano-silica composites	rigid	20	0.022	15
2019	AlN/Si(doped)	GO	rigid	221.2	25.3	25
2020	ST-quartz	SiO_2/3D grapheme/polyvinyl alcohol	rigid	202	1.44	14
2020	ZnO/flexible glass	ZnO NWs and GQDs	flexible	220.2	40.16	**This work**

[b)] the sensitivity at 80%RH.

where f_r is the resonant frequency, C is a constant and A is the sensing area. Therefore, the larger resonant frequency will lead to a larger frequency shift, thus increasing the sensitivity. The largest sensitivity value of 40.16 kHz/%RH was obtained from the flexible SAW device with the resonant frequency of ~220 MHz, which is much larger than the other reported SAW-based humidity sensors, as listed in Table 2. The resolutions of these SAW based humidity sensors resolution are better than 1% RH as shown in Figure S3.

To demonstrate the sensing performance when the SAW device is in a bent shape, we have fixed a flexible sensor (sample D7 listed in Table 1) onto metal support and bent it at an angle of 30°, as shown in Figure 6(a). Figure 6(b) shows the results of humidity sensing for this SAW sensor at both flat and bent conditions. The frequency shifts of the sensor for both two cases have a comparable humidity sensing performance, with a relative error of less than 2.5%.

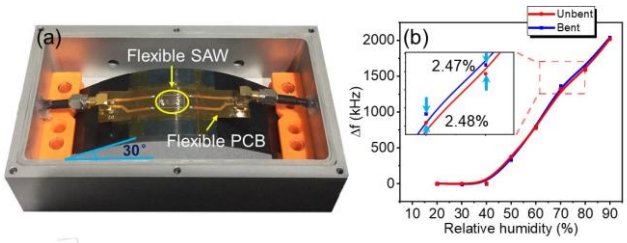

Figure 6. (a) Photograph of the sensor at a bent state; (b) Frequency shifts of a flexible humidity sensor (λ=12 μm, D7) for unbent condition and bent condition at an angle of 30°.

The wearable applications of the flexible SAW sensor have further been demonstrated. As shown in Figure 7(a), the flexible SAW sensor was placed on the wrist to detect the humidity change of environment. In these experiments, the atomizer was used to produce water molecules in order to simulate the humidity changes of environment around the body. Figure 7(b) shows the changes of resonant frequency of the flexible SAW sensor as a function of humidity change of environment. The resonant frequency of sensor is shifted downwards when the atomizer is switched on, which is due to the change in humidity levels. The sensor recovers to its original value when the atomizer is switched off. Five cycles of repeated monitoring of the humidity change of environment have also been conducted and the results demonstrated a good repeatability of the flexible SAW devices. In addition, the flexible SAW device was also used to detect the breath processes as shown in Figures 7(c) and 7(d). The frequency of the flexible humidity sensor decreases after exposure to breathing but then recovers to its original value for five cycles. These environment humidity tests and breathing tests demonstrate the suitable applications of flexible SAW device into the wearable electronics.

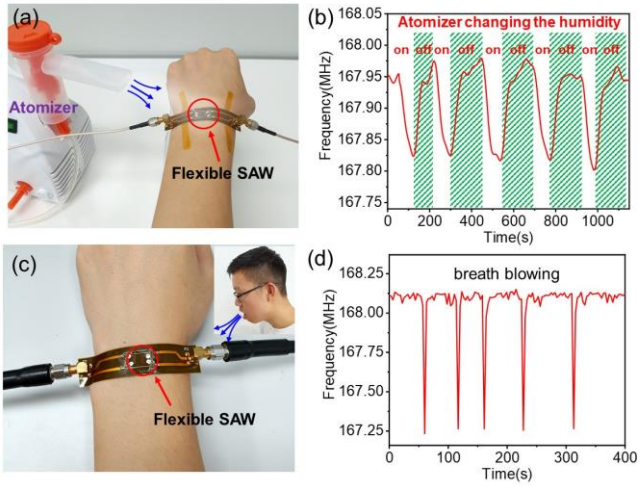

Figure 7. (a) Illustration of the experimental setup for the flexible SAW humidity sensor on wrist, and the atomizer to simulate humidity change of environment; (b) The resonant frequency shifts as a function of relative humidity in the environment for flexible SAW sensors with a wavelength of 16 μm; (c) Illustration of the experimental setup of the flexible SAW for breathing detection on wrist; (d) Resonant frequency

changes in the flexible SAW humidity sensor after five cycles of exposure to breathing with a SAW device wavelength of 16 μm;

Conclusions

In summary, we reported a highly flexible and ultra-sensitive ZnO/glass SAW humidity sensor with a composite sensitive layer of ZnO NWs and GQDs. The flexible SAW device has achieved a large effective electromechanical coupling coefficient of 3.5% and a large signal amplitude of 45 dB, which are ~400% and ~180% higher than those of the previously reported flexible ZnO/polymer SAW devices at the same configurations. The composite sensing layer can significantly improve the sensitivity of the flexible SAW devices, due to the large specific surfaces of ZnO NWs, large numbers of hydrophilic functional groups of GQDs, as well as the formation of p-n heterojunctions between GQDs and ZnO NWs. All these can significantly enhance the adsorption of water molecules. An ultra-high humidity sensitivity of 40.16 kHz/%RH was obtained with excellent stability and repeatability. We further demonstrated that the flexible SAW sensors functioned well without apparent performance deterioration when it was attached to the curved surface with bending angle of 30°. Finally we demonstrated the wearable applications for humidity sensing and human breathing detection, revealing the potential applications in human-machine interaction (HMI), spatial localization, and personal health care.

ASSOCIATED CONTENT

Supporting Information

Manufacturing process of the ZnO NWs/GQDs composite materials; Calculation of the specific surface area of ZnO NWs; Resolution test of the flexible SAW humidity sensor.

AUTHOR INFORMATION

Corresponding Author

* Jian Zhou, Ph. D
Professor in College of Mechanical and Vehicle Engineering
Engineering Research Center of Automotive Electrics and Control Technology
Hunan University, Changsha 410082, P.R. China
Email: jianzhou@hnu.edu.cn

Author Contributions

‡These authors contributed equally. The manuscript was written through contributions of all authors. All authors have given approval to the final version of the manuscript.

Notes

The authors declare no competing financial interests.

ACKNOWLEDGMENT

This work was supported by Key Research Project of Hunan Province (2019GK2111, 2018GK2044) and the UK Engineering and Physical Sciences Research Council (EPSRC EP/P018998/1). The authors acknowledge the State Key Laboratory of Advanced Design and Manufacturing for Vehicle Body, Hunan University.

REFERENCES

1. Blank, T. A.; Eksperiandova, L. P.; Belikov, K. N. Recent trends of ceramic humidity sensors development: A review. *Sens. Actuators B-Chem* **2016**, *228*, 416-442.
2. Anastasova, S.; Crewther, B.; Bembnowicz, P.; Curto, V.; Ip, H. M. D.; Rosa, B.; Yang, G. Z. A wearable multisensing patch for continuous sweat monitoring. *Biosens. Bioelectron.* **2017**, *93*, 139-145.
3. Duan, Z. H.; Jiang, Y. D.; Yan, M. G.; Wang, S.; Yuan, Z.; Zhao, Q. N.; Sun, P.; Xie, G. Z.; Du, X. S.; Tai, H. L. Facile, Flexible, Cost-Saving, and Environment-Friendly Paper-Based Humidity Sensor for Multifunctional Applications. *Acs Appl. Mater. Interfaces* **2019**, *11*, 21840-21849.
4. Pang, Q.; Lou, D.; Li, S. J.; Wang, G. M.; Qiao, B. B.; Dong, S. R.; Ma, L.; Gao, C. Y.; Wu, Z. H. Smart Flexible Electronics-Integrated Wound Dressing for Real-Time Monitoring and On-Demand Treatment of Infected Wounds. *Adv. Sci.* **2020**, *7*, 1902673.
5. Xu, K. C.; Lu, Y. Y.; Takei, K. Multifunctional Skin-Inspired Flexible Sensor Systems for Wearable Electronics. *Adv. Mater. Technol.* **2019**, *4*, 1800628.
6. Yang, J. H.; Shi, R. L.; Lou, Z.; Choi, R. Q.; Jiang, K.; Shen, G. Z. Flexible Smart Noncontact Control Systems with Ultrasensitive Humidity Sensors. *Small* **2019**, *15*, 1902801.
7. Wang, Y.; Zhang, L. N.; Zhou, J. P.; Lu, A. Flexible and Transparent Cellulose-Based Ionic Film as a Humidity Sensor. *Acs Appl. Mater. Interfaces* **2020**, *12*, 7631-7638.
8. Choi, J. W.; Kwon, S. H.; Huh, C. H.; Park, K. C.; Youn, S. W. The influences of skin visco-elasticity, hydration level and aging on the formation of wrinkles: a comprehensive and objective approach. *Skin Res. Technol.* **2013**, *19*, E349-E355.
9. Lamanna, L.; Rizzi, F.; Guido, F.; Algieri, L.; Marras, S.; Mastronardi, V. M.; Qualtieri, A.; De Vittorio, M. Flexible and Transparent Aluminum-Nitride-Based Surface-Acoustic-Wave Device on Polymeric Polyethylene Naphthalate. *Adv. Electron. Mater.* **2019**, *5*, 1900095.
10. Xu, H. S.; Dong, S. R.; Xuan, W. P.; Farooq, U.; Huang, S. Y.; Li, M. L.; Wu, T.; Jin, H.; Wang, X. Z.; Luo, J. K. Flexible surface acoustic wave strain sensor based on single crystalline LiNbO3 thin film. *Appl. Phys. Lett.* **2018**, *112*, 093502.
11. Chen, Z.; Zhou J.; Tang, H.; Liu, Y.; Shen, Y.P.; Yin, X.B.; Zheng, J. P.; Zhang, H.S.; Wu, J. H.; Shi, X.L.; Chen, Y.Q.; Fu, Y.Q.; Duan, H.G. Ultrahigh-Frequency Surface Acoustic Wave Sensors with Giant Mass-Loading Effects on Electrodes. *ACS Sens.* **2020**, *5, 1657-1664*.
12. Jin, H.; Zhou, J.; He, X.; Wang, W.; Guo, H.; Dong, S.; Wang, D.; Xu, Y.; Geng, J.; Luo, J. K.; Milne, W. I. Flexible surface acoustic wave resonators built on disposable plastic film for electronics and lab-on-a-chip applications. *Sci. Rep.* **2013**, *3*, 2140.
13. Li, Y.; Li, P.; Yang, M.; Lei, S.; Chen, Y.; Guo, X. A surface acoustic wave humidity sensor based on electrosprayed silicon-containing polyelectrolyte. *Sens. Actuators B-Chem* **2010**, *145*, 516-520.
14. Su, Y.; Li, C.; Li, M.; Li, H.; Xu, S.; Qian, L.; Yang, B. Surface acoustic wave humidity sensor based on three-dimensional architecture graphene/PVA/SiO2 and its application for respiration monitoring. *Sens. Actuators B-Chem* **2020**, *308*, 127693.
15. Zheng, X.; Fan, R.; Li, C.; Yang, X.; Li, H.; Lin, J.; Zhou, X.; Lv, R. A fast-response and highly linear humidity sensor based on quartz crystal microbalance. *Sens. Actuators B-Chem* **2019**, *283*, 659-665.
16. Li, D. J.; Zhao, C.; Fu, Y. Q.; Luo, J. K. Engineering Silver Nanostructures for Surface Acoustic Wave Humidity Sensors Sensitivity Enhancement. *J. Electrochem. Soc.* **2014**, *161*, B151-B156.
17. Hong, H. S.; Chung, G. S. Controllable growth of oriented ZnO nanorods using Ga-doped seed layers and surface acoustic wave humidity sensor. *Sens. Actuators B-Chem* **2014**, *195*, 446-451.
18. He, X. L.; Li, D. J.; Zhou, J.; Wang, W. B.; Xuan, W. P.; Dong, S. R.; Jin, H.; Luo, J. K. High sensitivity humidity sensors using flexible surface acoustic wave devices made on nanocrystalline ZnO/polyimide substrates. *J. Mater. Chem. C* **2013**, *1*, 6210-6215.
19. Jin, H.; Tao, X.; Dong, S. R.; Qin, Y. H.; Yu, L. Y.; Luo, J. K.; Deen, M. J. Flexible surface acoustic wave respiration sensor for monitoring obstructive sleep apnea syndrome. *J. Micromech. Microeng.* **2017**, *27*, 115006.
20. Fu, Y. Q.; Luo, J. K.; Nguyen, N. T.; Walton, A. J.; Flewitt, A. J.; Zu, X. T.; Li, Y.; McHale, G.; Matthews, A.; Iborra, E.; Du, H.; Milne, W. I. Advances in piezoelectric thin films for acoustic biosensors, acoustofluidics and lab-on-chip applications. *Prog. Mater. Sci.* **2017**, *89*, 31-91.

21. Tao, X.; Jin, H.; Mintken, M.; Wolff, N.; Wang, Y.; Tao, R.; Li, Y.; Torun, H.; Xie, J.; Luo, J.; Zhou, J.; Wu, Q.; Dong, S.; Luo, J.; Kienle, L.; Adelung, R.; Mishra, Y. K.; Fu, Y. Q. Three-Dimensional Tetrapodal ZnO Microstructured Network Based Flexible Surface Acoustic Wave Device for Ultraviolet and Respiration Monitoring Applications. *Acs Appl. Nano Mater.* **2020**, *3*, 1468-1478.

22. Xu, W. J.; Bai, Y. C.; Yin, Y. D. Surface Engineering of Nanostructured Energy Materials. *Adv. Mater.* **2018**, *30*, 1802091.

23. Wang, Z. L. Characterizing the structure and properties of individual wire-like nanoentities. *Adv. Mater.* **2000**, *12*, 1295-+.

24. Xuan, W.; He, X.; Chen, J.; Wang, W.; Wang, X.; Xu, Y.; Xu, Z.; Fu, Y. Q.; Luo, J. K. High sensitivity flexible Lamb-wave humidity sensors with a graphene oxide sensing layer. *Nanoscale* **2015**, *7*, 7430-7436.

25. Le, X.; Liu, Y.; Peng, L.; Pang, J.; Xu, Z.; Gao, C.; Xie, J. Surface acoustic wave humidity sensors based on uniform and thickness controllable graphene oxide thin films formed by surface tension. *Microsyst. Nanoeng.* **2019**, *5*, 36.

26. Traversa, E. Ceramic sensors for humidity detection: the state-of-the-art and future developments. *Sens. Actuators B-Chem* **1995**, *23*, 135-156.

27. Alizadeh, T.; Shokri, M. A new humidity sensor based upon graphene quantum dots prepared via carbonization of citric acid. *Sens. Actuators B-Chem* **2016**, *222*, 728-734.

28. Miller, D. R.; Akbar, S. A.; Morris, P. A. Nanoscale metal oxide-based heterojunctions for gas sensing: A review. *Sens. Actuators B-Chem* **2014**, *204*, 250-272.

29. Zhang, Y.; Zou, H. F.; Peng, J. F.; Duan, Z. H.; Ma, M.; Xin, X.; Li, W. L.; Zheng, X. J. Enhanced humidity sensing properties of SmFeO3-modified MoS2 nanocomposites based on the synergistic effect. *Sens. Actuators B-Chem* **2018**, *272*, 459-467.

30. Yang, Z. L.; Zhang, Z. Y.; Liu, K. C.; Yuan, Q.; Dong, B. Controllable assembly of SnO2 nanocubes onto TiO2 electrospun nanofibers toward humidity sensing applications. *J. Mater. Chem. C* **2015**, *3*, 6701-6708.

31. Nair, S. S.; Illyaskutty, N.; Tam, B.; Yazaydin, A. O.; Emmerich, K.; Steudel, A.; Hashem, T.; Schottner, L.; Woll, C.; Kohler, H.; Gliemann, H. ZnO@ZIF-8: Gas sensitive core-shell hetero-structures show reduced cross-sensitivity to humidity. *Sens. Actuators B-Chem* **2020**, *304*, 127184.

32. Dang, W. L.; Fu, Y. Q.; Luo, J. K.; Flewitt, A. J.; Milne, W. I. Deposition and characterization of sputtered ZnO films. *Superlattices Microstruct.* **2007**, *42*, 89-93.

33. Mani, G. K.; Morohoshi, M.; Yasoda, Y.; Yokoyama, S.; Kimura, H.; Tsuchiya, K. ZnO-Based Microfluidic pH Sensor: A Versatile Approach for Quick Recognition of Circulating Tumor Cells in Blood. *Acs Appl. Mater. Interfaces* **2017**, *9*, 5193-5203.

34. Khorsand Zak, A.; Abd. Majid, W. H.; Abrishami, M. E.; Yousefi, R. X-ray analysis of ZnO nanoparticles by Williamson-Hall and size-strain plot methods. *Solid State Sci.* **2011**, *13*, 251-256.

35. Tuteja, S. K.; Chen, R.; Kukkar, M.; Song, C. K.; Mutreja, R.; Singh, S.; Paul, A. K.; Lee, H.; Kim, K. H.; Deep, A.; Suri, C. R. A label-free electrochemical immunosensor for the detection of cardiac marker using graphene quantum dots (GQDs). *Biosens. Bioelectron.* **2016**, *86*, 548-556.

36. Ming, H.; Ma, Z.; Liu, Y.; Pan, K. M.; Yu, H.; Wang, F.; Kang, Z. H. Large scale electrochemical synthesis of high quality carbon nanodots and their photocatalytic property. *Dalton Trans.* **2012**, *41*, 9526-9531.

37. Xiong, S.; Liu, X. D.; Zhou, J.; Liu, Y.; Shen, Y. P.; Yin, X. B.; Wu, J. H.; Tao, R.; Fu, Y. Q.; Duan, H. G. Stability studies of ZnO and AlN thin film acoustic wave devices in acid and alkali harsh environments. *RSC Adv.* **2020**, *10*, 19178-19184.

38. Kannan, P. K.; Saraswathi, R.; Rayappan, J. B. B. A highly sensitive humidity sensor based on DC reactive magnetron sputtered zinc oxide thin film. *Sens. Actuators, A* **2010**, *164*, 8-14.

39. Ballantine, D.; White, R.; Martin, S.; Ricco, A.; Zellers, E.; Frye, G.; Wohltjen, H. *Acoustic wave sensors, theory, design, and physico-chemical applications*. Academic: San Diego, 1997.

40. Bondarenka, V.; Grebinskij, S.; Mickevičius, S.; Volkov, V.; Zacharova, G. Thin films of poly-vanadium-molybdenum acid as starting materials for humidity sensors. *Sens. Actuators B-Chem* **1995**, *28*, 227-231.

41. Qi, Q.; Zhang, T.; Yu, Q.; Wang, R.; Zeng, Y.; Liu, L.; Yang, H. Properties of humidity sensing ZnO nanorods-base sensor fabricated by screen-printing. *Sens. Actuators B-Chem* **2008**, *133*, 638-643.

42. Tang, Y.; Li, Z.; Ma, J.; Wang, L.; Yang, J.; Du, B.; Yu, Q.; Zu, X. Highly sensitive surface acoustic wave (SAW) humidity sensors based on sol-gel SiO2 films: Investigations on the sensing property and mechanism. *Sens. Actuators B-Chem* **2015**, *215*, 283-291.

43. Le, X.; Wang, X.; Pang, J.; Liu, Y.; Fang, B.; Xu, Z.; Gao, C.; Xu, Y.; Xie, J. A high performance humidity sensor based on surface acoustic wave and graphene oxide on AlN/Si layered structure. *Sens. Actuators B-Chem* **2018**, *255*, 2454-2461.

SYNOPSIS TOC